The Dhaka University Journal of Earth and Environmental Sciences, Vol. 14 (1): 2025

Spatiotemporal Analysis of Land Use-Land Cover Changes in Pleistocene Uplifted Madhupur Tract Region using Geospatial Techniques

Md. Mainul Islam, Md. Bodruddoza Mia* and Md. Nasif Jamil

Department of Geology, University of Dhaka, Dhaka 1000, Bangladesh

Manuscript received: 05 November 2024; accepted for publication: 05 March 2025

ABSTRACT: The Madhupur Tract region of Bangladesh, characterized by Pleistocene uplifted terrain, is undergoing rapid and unplanned urbanization, marked by increased population density, industrial expansion, and infrastructure development. To highlight the environmental effects of urbanization on this previously unexplored region, this study uses geospatial approaches to assess the spatiotemporal changes in land use and land cover (LULC) in the Madhupur Tract. Utilizing multispectral Landsat images from 2000, 2010 and 2023, LULC maps were generated using unsupervised classification methods in ArcGIS. Indices such as the Normalized Difference Vegetation Index (NDVI), Normalized Difference Water Index (NDWI), and Normalized Difference Built-up Index (NDBI) were employed to evaluate land cover dynamics and spatial patterns for the years 2000,2005, 2010, 2015 and 2023. Results revealed significant land cover changes over the study period, with a marked decline in forest cover and agricultural land and a substantial increase in settlement areas due to urban growth. From 2000 to 2023, forest cover decreased from 29% to 11%, while settlements expanded from 10% to 30%, indicating extensive urbanization and deforestation. NDVI analysis showed fluctuations in vegetation health, with sparse vegetation decreasing and barren land increasing significantly, reflecting ongoing land degradation. NDWI results indicated a dramatic reduction in water bodies, declining from 30% coverage in 2000 to just 6% in 2023. The findings of this study provide critical insights into the complex interplay between urban expansion and environmental degradation within the Madhupur Tract, emphasizing the region's vulnerability to unsustainable development practices. By documenting the loss of natural landscapes and the intensification of built-up areas, this research highlights the urgent need for integrating sustainable land management and urban planning policies to balance economic development with environmental conservation.

Keywords: Landuse-Landcover; Urbanization; Madhupur Tract; Landsat Images; Geospatial Techniques

INTRODUCTION

Urbanization is frequently associated with socioeconomic progress and poverty alleviation, but it also leads to permanent changes in biodiversity and land use. This transformation can result in the loss of agricultural land, disruption of terrestrial carbon reservoirs, threats to biodiversity, altered hydrological systems, and impacts local and regional climates. Urbanization predominantly reflects variations in land use and is considered by researchers to be a principal cause of climate change and ecological diversity (Ding and Shi, 2013). The rapid shift from rural to urban areas through industrialization is one of the fastest transformations in recent history, significantly impacting the natural functioning of ecosystems. Urban expansion causes unsustainable development, especially due to the rapid reduction in vegetation cover driven by changing land-use and land-cover (LULC) dynamics (Adegboyega et al., 2019). The transformation of LULC profoundly affects biodiversity and ecosystems (Luck and Wu, 2002), and both natural processes and anthropogenic activities continuously alter surface morphology, land cover, and land use (Alam et al., 2022). The impacts of LULC on climate exhibit substantial regional variations (Vermeulen et al., 2012). Additionally, land use plays a significant role in climate change, as deforestation contributes to greenhouse gas (GHG) emissions, while climate change, in turn, influences future land cover and agricultural productivity (Dissanayake et al., 2017). Over the past 150 years, nearly one-third of the CO2 emitted has been attributed to LULC changes (Edenhofer, 2015).

The physiographic unit, Madhupur Tract of Bangladesh is facing numerous environmental challenges due to factors such as population growth, unplanned urbanization, booming garment factories and the drying

*Corresponding author: Md. Bodruddoza Mia

Email: bodruddoza@du.ac.bd

DOI: https://doi.org/10.3329/dujees.v14i1.83013

up of river channels. As this region intersects with a highly extensive economic zone, these pressures are exacerbating the area's natural hazards and human impacts. For instance, Yesmin et al. (2014) used remote sensing and GIS techniques to document land-use and land-cover changes over 20 years in Gazipur District, revealing the construction of numerous factories and rapid population growth, which has intensified deforestation. The Madhupur Sal Forest, one of Bangladesh's most ecologically significant and productive forest types, is currently undergoing severe destruction. Over the past 30 years, the area of the Sal Forest has decreased by 23.35%, while settlements and bare land have increased by 107.19% and 160.89%, respectively (Islam et al., 2023). The growing population in this region also generates large amounts of waste, leading to landfills, pollution, deforestation, and the filling of water bodies for settlement and development purposes. This rapidly changing environment highlights the need for effective monitoring and management strategies.

Remote sensing data provides essential information about land use and its changes over time, offering insights that are critical for a variety of applications such as environmental protection, forestry, hydrology, agriculture, and geology (Al Faruq et al., 2016). These techniques are indispensable for detecting and managing environmental and meteorological phenomena (Borges et al., 2016). Access to historical and current land cover information is vital for sustainable management practices (Chaurasia et al., 1996). LULC classification provides valuable data on urban areas, agricultural lands, vegetation, natural surfaces, and cultural features (Akinci et al., 2013). Furthermore, LULC data are crucial inputs for climate-change-related models, particularly those that are policy-oriented (Disperati and Virdis, 2015). The regional impacts of LULC on climate are significant and vary across different regions (Vermeulen et al., 2012). Remote sensing remains one of the most accurate methods for detecting changes in vegetation cover (Miller et al., 1998). The Normalized Difference Vegetation Index (NDVI), derived from satellite imagery, has become a standard tool for estimating vegetation productivity (Rouse et al., 1974). Additionally, the Modified Normalized Difference Water Index (MNDWI), developed by Xu (2006), is used to detect changes in water content and purity. By applying appropriate threshold values, these indices are instrumental in classifying different LULC types (Chen et al., 2006).

The primary objective of this research is to analyze the spatio-temporal variability of land use and land cover (LULC) changes, focusing on an area that has received limited prior study. Specifically, this research seeks to identify and assess the impacts of rapid urbanization on LULC, including patterns of urban growth, land cover loss, and associated environmental factors. By leveraging satellite remote sensing, this study will generate thematic maps representing various land cover types—such as water bodies, forests, and settlements—while evaluating spatial patterns using indices like NDVI, NDWI, and NDBI. Additionally, a time series analysis from 2000 to 2023 will offer insights into the dynamics of these changes.

STUDY AREA

The Madhupur Tract Region (Fig. 1) area is in the Middle part of Bangladesh i.e., Dhaka & Mymensingh division. Mymensingh division was formerly part of Dhaka division. It was declared as Bangladesh's 8TH division. The Madhupur Ghar is situated in Tangail & Gazipur which is in Dhaka division & rest part lies in Mymensingh including Jamalpur in north Mymensingh in northeast. The total extent of this Madhupur Tract is 4,244 km^2 (Banglapedia, 2023*)*. Madhupur hill track is considered as Pleistocene upland which has distinct characteristics of reddish fine grain soil with many muds' balls & tree trunks. Highly oxidize soil special characteristic of this area which may help special type of tree called Sal (Mizanur et al., 2009). Later Pleistocene monsoon climatic periods induced massive current movement across the Bengal plain, resulting in the dissection of the original Madhupur surface. As monsoon rainfall intensified, the valleys created by this erosion accumulated sediments of Holocene epoch, creating a geomorphic level positioned lower than the original surface (Rashid, T., 2014).

MATERIALS AND METHODS

Satellite Images

For this research, satellite images were obtained for free from the United States Geological Survey (USGS) (https://earthexplorer.usgs.gov) database. Five sets of Landsat images with same path and row were gathered from the USGS website in GeoTIFF format to cover the study region (Madhupur Unit) for the years 2000, 2005, 2010, 2015, and 2023 (Table 1). Three image sets were required to cover the full research area.

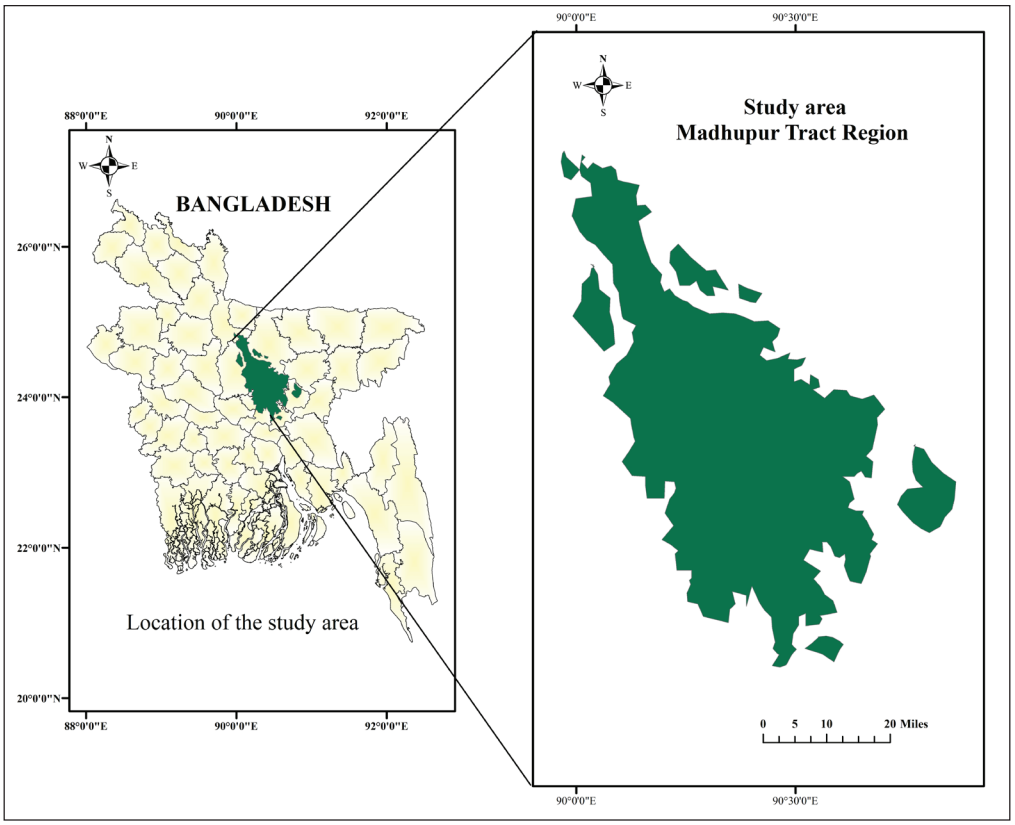

Figure 1: Geographic Location and Extent of the Study Area (Madhupur Tract Region**)**

The Landsat images which are used in research were projected as Universal Transverse Mercator (UTM) zone 45N using the Datum World Geodetic System (WGS) 1984. For the availability of sun, just daytime images were gathered for optimal result. At the exact same time intervals Landsat images could not have gathered due to fresh, spotlessness and images of low cloud cover (<10%) within the desired path and rows. The selection of November for 2005 and January/February for subsequent years was based on data availability and consistency in sampling during the dry season. These months represent similar hydrological conditions critical for our analysis. Images which have been obtained from the United States Geological Survey (USGS) archive are listed in table 1.

Table 1: Landsat Images Used in the Study

Year	Sensor Platform	Acquisition Date	WRS Path and Row	Resolution
2000	Landsat-7	28th February,2000	137,43	30 m
2005	Landsat-5	16th November,2005	137,43	30 m
2010	Landsat-5	30th January, 2010	137,43	30 m
2015	Landsat-8	28th January, 2015	137,43	30 m
2023	Landsat-8	2ndFebruary,2023	137,43	30 m

METHODOLOGY

Image Pre-Processing

Four images (2000, 2005, 2010, 2015 and 2023) of Landsat level-1 data were collected from USGS Earth Explorer for this study. Raw Landsat images are geometrically corrected but often contain radiometric errors. Radiometric distortions arise because of a poorly clear atmosphere, daily and seasonal fluctuations in the amount of solar radiation absorbed at the ground level, and flaws in scanning apparatus. Hence the image data are corrected to create a more authentic representation of the original scene.

Radiometric Correction

Radiometric correction need for comparing multiple data sets over a long period of time as it helps to nullify the effects that modify the spectral characteristics of land features (Paolini et al., 2006). It aids in calibrating pixel values and rectifying errors in the data, thereby enhancing the interpretability and quality of remote sensing data. The Digital Number (DN) is intensity of the electromagnetic radiation for each pixel is recorded by the sensor which can be translated into more practical real-world units such as radiance, reflectance, and brightness temperature. Sensor-specific data is required for this validation procedure, which can be obtained from the metadata files of Landsat photos. For radiometric validation, the DN value from sensor data is translated into at-sensor radiance and top-of-atmosphere reflectance (TOA). In the end, atmospheric correction is done by using dark object subtraction method.

Layer stack, Mosaic and Subset

Several bands of acquisition sensors were combined after collection of the images by "Layer stacking" process. For layer stacking process, it needs having band of same spatial resolution. Therefore, all the bands without the "Thermal" and "panchromatic" are combined. Individual land surface features can be better identified with true and false color composite map of the layer stacked image. Then further analysis operated in this study area

Unsupervised Classification Based LULC Mapping

Landsat TM, ETM+, and OLI/TIRS images from the years 2000, 2010, and 2023 were used to prepare LULC maps using the unsupervised classification method. ArcGIS software facilitated the classification process (Fig. 2). The unsupervised approach was selected primarily due to the lack of sufficient field-specific data necessary to create accurate signatures for specific classes. The classification was based on the spectral characteristics of the images, and all classes were manually labeled to meaningful land cover categories. In some cases, a single land cover type was represented by multiple clusters; these clusters were merged into a single class using the "Recode" process.

Accuracy Assessment

To distinguish true land cover changes from potential classification errors, error matrices and per-class accuracy indices were calculated for the year 2023. In this assessment, 100 stratified random points were generated across the study area using high-resolution imagery to determine the actual land use and land cover (LULC) classes. These verified classes, derived from the reference images, were then utilized to evaluate per-class accuracy (i.e., user's and producer's accuracy). Additionally, overall accuracy and the Kappa coefficient for the year were computed to provide a comprehensive evaluation of the classification performance.

Producer's Accuracy (PA): Measures how well a particular land cover class has been classified from the perspective of the classifier (or producer). It indicates the probability that a reference pixel (ground truth) is correctly classified in the map.

User's Accuracy (UA): Measures the accuracy from the user's perspective, demonstrating how often the class on the map accurately represents the real-world category.

Normalized Difference Vegetation Index (NDVI) Retrieval

The Normalized Difference Vegetation Index (NDVI) quantifies vegetation by comparing the difference between near-infrared light, which is strongly reflected by vegetation, and red light, which is absorbed by vegetation (Carlson et al., 1997). Very low values of correspond to water body (Gandhi et al., 2015). In NDVI imagery, vegetated areas appear as lighter tones, while non-vegetated areas appear as darker tones. The NDVI can be calculated using the following equation, as proposed by Rouse et al. (1974):

$$\mathbf{NDVI} = \frac{NIR - RED}{NIR + RED}$$

Here, "RED = Reflectance Red region of the multispectral image & NIR = Reflectance of Near Infra-Red region of the multispectral image"

The value of NDVI ranges between -1 to +1. Dense vegetation areas show positive values close to +1 whereas snow, cloud and water body show lower values close to -1. For Landsat 5 (TM) and Landsat 7 (ETM^{+}), band 4 and band 3 represent the NIR and RED region respectively.

$$\mathbf{NDVI} = \frac{\boldsymbol{Band\ 4 - Band\ 3}}{\boldsymbol{Band\ 4 + Band\ 3}}$$ (For Landsat 5 and 7)

On the other hand, for Landsat 8, the reflectance values of band 5 and band 4 represent NIR and RED region is used to retrieve NDVI thematic maps of the study area as below.

$$\mathbf{NDVI} = \frac{\boldsymbol{Band\ 5 - Band\ 4}}{\boldsymbol{Band\ 5 + Band\ 4}}$$ (For Landsat 8)

Normalized Difference Water Index (NDWI) Retrieval

Using Normalized Difference Water Index (NDWI) methods detect changes related to water content in water bodies. The index is designed to maximize the high reflectance of water by using green wavelengths and minimize the low reflectance by NIR bands (Xu, 2006). It also uses the advantage of high reflectance of NIR by vegetation and soil features. NDWI can be calculated using the following equation defined by McFeeters (1996):

$$\mathbf{NDWI} = \frac{\mathbf{GREEN} - \boldsymbol{NIR}}{\boldsymbol{GREEN + NIR}}$$

Here, "GREEN = Reflectance of the Green region of the multispectral image &

NIR = Reflectance of the Near Infra- Red region of the multispectral image"

NDWI values vary from -1 to +1. Here positive values indicate features like water, which are intensified whereas negative values indicate vegetation and soil. For Landsat 5(TM) and Landsat 7 (ETM^+), band 2 and band 4 represents Green and NIR region respectively.

$$\mathbf{NDWI} = \frac{\boldsymbol{Band\ 2 - Band\ 4}}{\boldsymbol{Band\ 2 + Band\ 4}}$$ (For Landsat 5 and 7)

In Landsat 8, "Band 3" and "Band 5" represent Green and NIR region respectively.

$$\mathbf{NDWI} = \frac{\boldsymbol{Band\ 3 - Band\ 5}}{\boldsymbol{Band\ 3 + Band\ 5}}$$ (For Landsat 8)

Normalized Difference Built-up Index (NDBI) Retrieval

For calculating Normalized Difference Built-up Index (NDBI), we need to use the "NIR" and "SWIR" bands to identify manufactured built-up areas. The method is based on ratios to reduce the impact of atmospheric factors and variations in terrain illumination.

$$\mathbf{NDBI} = \frac{\mathbf{(SWIR - NIR)}}{\mathbf{(SWIR + NIR)}}$$

Here, "NIR = Reflectance of the Near Infra- Red region of the multispectral image & SWIR = Shortwave Infrared Band"

The NDBI values vary from -1 to 1. High NDBI values represent the built-up areas whereas low NDBI values represent the other regions. For Landsat 5(TM) and Landsat 7 (ETM^+), band 5 and band 4 represent SWIR and NIR region respectively.

$$\mathbf{NDBI} = \frac{\boldsymbol{Band\ 5 - Band\ 4}}{\boldsymbol{Band\ 5 + Band\ 4}}$$ (For Landsat 5 and 7)

But in Landsat 8, Band 6 and band 5 represent SWIR and RED region.

$$\mathbf{NDBI} = \frac{\boldsymbol{Band\ 6 - Band\ 5}}{\boldsymbol{Band\ 6 + Band\ 5}}$$ (For Landsat 8)

RESULTS

Landuse-Landcover (LULC) Mapping

The unsupervised classified thematic images (Fig. 3) of the years 2000, 2010, and 2023 have been utilized for the detecting the changes (Table 2) in land use and land cover in the study area. Waterbody, forest, agricultural land, bare land and settlement have been identified as spectral classes.

In 2000, the LULC analysis revealed a diverse landscape with water bodies covering 20% (8324.29 sq km), forests at 29% (12376.3 sq km), and agricultural land occupying 33% (13810 sq km), highlighting extensive farming. Bare land made up 8% (3554.24 sq km), reflecting areas with little vegetation, while settlements, including urban areas, covered 10% (4181.72 sq km). In 2010, the LULC analysis indicated significant landscape changes from 2000. Water bodies slightly decreased to 19% (8086.73 sq km), while forests reduced to 15% (6490.52 sq km), suggesting deforestation. Agricultural land shrank to 21% (8793.18 sq km), and bare land expanded to 23% (9587.87 sq km), indicating increased areas with minimal vegetation. Settlements grew significantly, covering 22% (9288.25 sq km), reflecting notable urbanization and infrastructure development. In 2023, the LULC analysis revealed significant landscape changes. Water bodies expanded to 22% (9282.55 sq km), indicating possible increases in lakes or water conservation. Forests decreased sharply to 11% (4444 sq km), suggesting deforestation or land conversion.

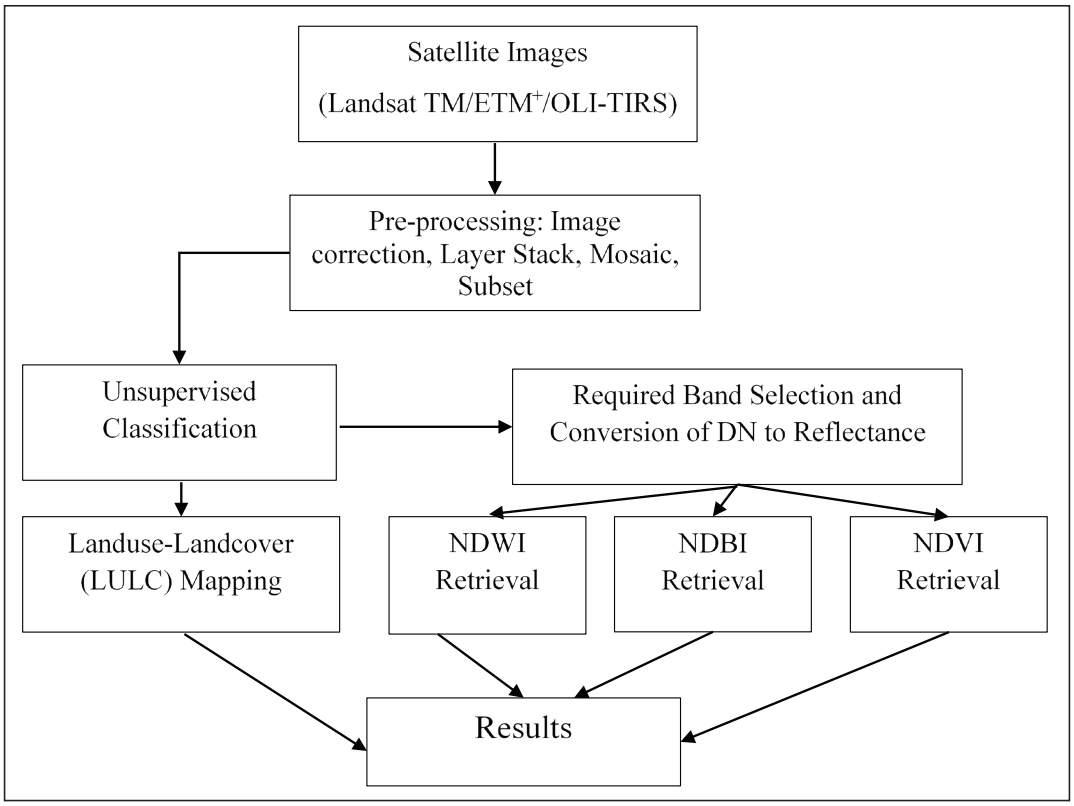

Figure 2: Flow Chart of the Research Methodology

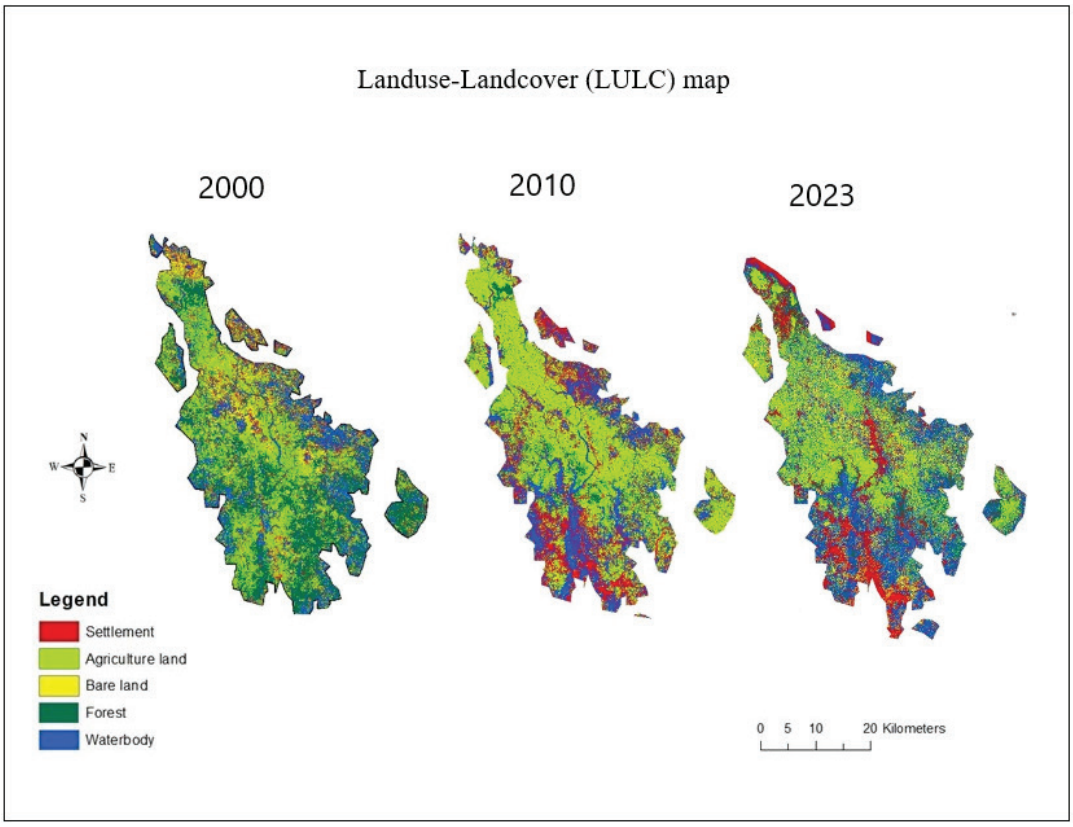

Figure 3: Landuse-Landcover (LULC) Map of the Research Area Using Unsupervised Classification for 2000, 2010 & 2023

Table 2: Area Coverage for Different Types of Land Cover in Different Years (sq km)

LULC types	Area Coverage in different years (sq km)		
	2000	**2010**	**2023**
Water body	8324.29	8086.73	9282.55
Forest	12376.3	6490.52	4444
Agricultural Land	13810	8793.18	9764
Bare Land	3554.24	9587.87	6232
Settlement	4181.72	9288.25	12524

Agricultural land remained stable at 23% (9764 sq km), continuing as a primary land use. Bare land increased to 15% (6232 sq km), reflecting further expansion of areas with minimal vegetation. Settlements grew substantially, covering 30% (12524 sq km), indicating considerable urbanization and infrastructure development (Fig. 4).

Accuracy Assessment

Table 3 presents the results from the per-class accuracy assessment for the year 2023. Most land cover classes exhibited user's accuracy (UA) and producer's accuracy (PA) values ranging between 50% and 90%. The waterbody and settlement classes achieved strong accuracies, with both classes attaining a user's accuracy of 90%.

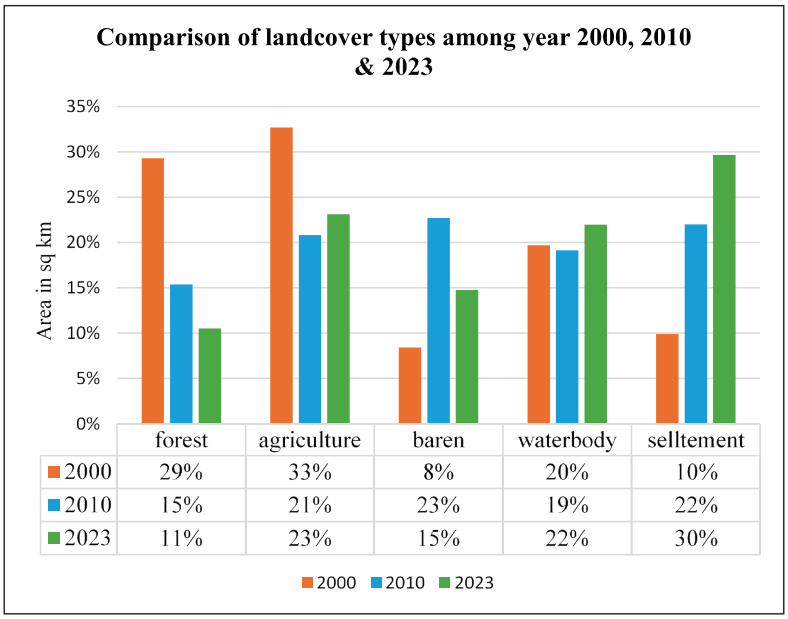

Figure 4: Graphical Representation Comparing the Landcover Types in Years 2000, 2010 & 2023

However, the agricultural land class displayed lower accuracies, with a producer's accuracy of only 58%, indicating potential misclassification or confusion with other land cover types. Additionally, the bare land class exhibited a user's accuracy of 72% and a producer's accuracy of 53%, likely reflecting its sparse distribution in the study area. Despite these variations, the overall accuracy for the classification was 92%, coupled with a Kappa coefficient of 0.825, suggesting near perfect agreement between the classified data and the reference data.

Table 3: Per-Class Accuracy Assessments of Multi-Temporal for the Year 2023

LULC Class	Year 2023	
	User's Accuracy (UA)	Producer's Accuracy (PA)
Waterbody	0.90	0.90
Forest	0.66	0.80
Agricultural Land	0.50	0.58
Bare Land	0.72	0.53
Settlement	0.90	0.64
overall accuracy	0.92	
Kappa coefficient	0.825	

LULC Mapping based on NDVI

The NDVI images (Fig. 5) identified four LULC types: water bodies, forests, agricultural land, and mixed land (including settlements, bare land, and some agricultural areas). Mixed land is represented by NDVI values greater than 0, moderate values (0.2 to 0.4) indicate agricultural land, and values above 0.4 signify healthy vegetation and forests. From 2000 to 2023, notable changes in these land cover types were observed. In 2000, water bodies covered approximately 6,152.8 sq km, barren land 1,098.8 sq km, sparse vegetation 21,191.3 sq km, and dense vegetation 13,810.3 sq km. By 2005, water bodies slightly expanded to 6,279 sq km, barren land increased to 1,977.8 sq km, sparse vegetation decreased to 13,442.8 sq km, and dense vegetation grew to 20,562 sq km. In 2010, water bodies remained stable at 6,176 sq km, barren land increased substantially to 18,090 sq km, sparse vegetation decreased to 17,795 sq km, and dense vegetation dropped to 275 sq km. By 2015, water bodies expanded to 7,682.9 sq km, barren land increased to 21,557.4 sq km, sparse vegetation reduced to 13,212.7 sq km, and dense vegetation decreased further to 324.9 sq km. Finally, by 2023, water bodies reached 7,975.6 sq km, barren land stabilized at 21,455.7 sq km, sparse vegetation declined to 12,798 sq km, and dense vegetation slightly increased to 551 sq km. Overall, the data reflects significant changes in land cover, with notable fluctuations in vegetation and an increase in water bodies and barren land over time (Table 4).

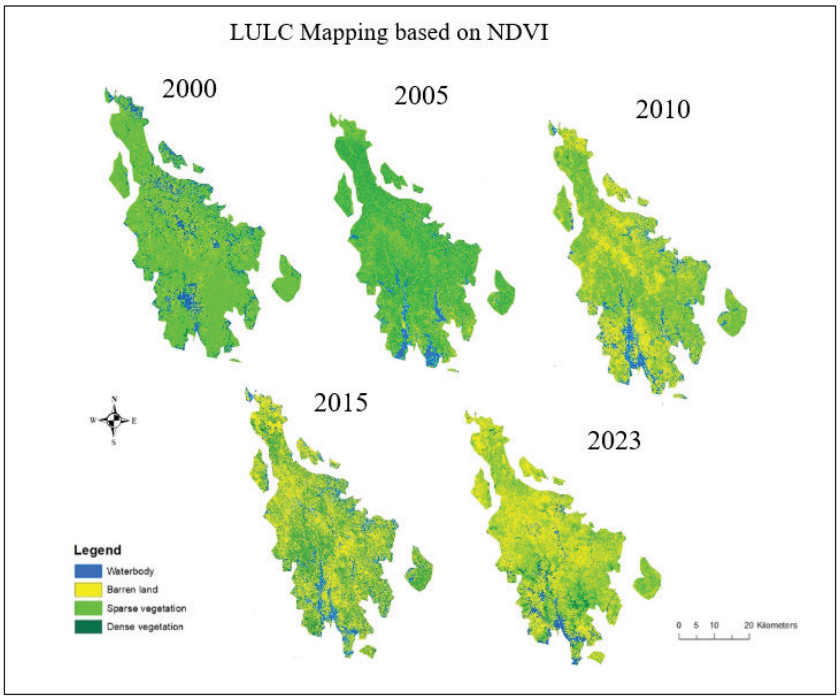

Figure 5: Landuse-Landcover (LULC) Map of the Research Area Using NDVI Classification (2000, 2005, 2010, 2015 & 2023)

Water bodies fluctuated, initially declining from 20% (8324.29 sq km) in 2000 to 19% in 2010 but then increasing to 22% (9282.55 sq km) in 2023. Forests saw a continuous decline, from 29% (12376.3 sq km) in 2000 to just 11% (4444 sq km) in 2023. Agricultural land, initially covering 33% (13810 sq km) in 2000, decreased to 21% in 2010 but rebounded slightly to 23% (9764 sq km) by 2023. Bare land expanded significantly from 8% (3554.24 sq km) in 2000 to 23% in 2010, reducing to 15% (6232 sq km) in 2023. Settlements grew markedly, expanding from 10% (4181.72 sq km) in 2000 to 30% (12524 sq km) in 2023 (Fig. 6).

Table 4: NDVI Classes for the Five Years with Area in Km²

Class Name	2000	2005	2010	2015	2023
Waterbody	6152.814	6278.967	6176	7682.913	7975.557
Barren land	1098.783	1977.786	18090	21557.4	21455.7
Sparse Vegetation	21191.29	13442.8	17795	13212.67	12797.98
Dense Vegetation	13810.29	20561.99	275	324.855	550.962

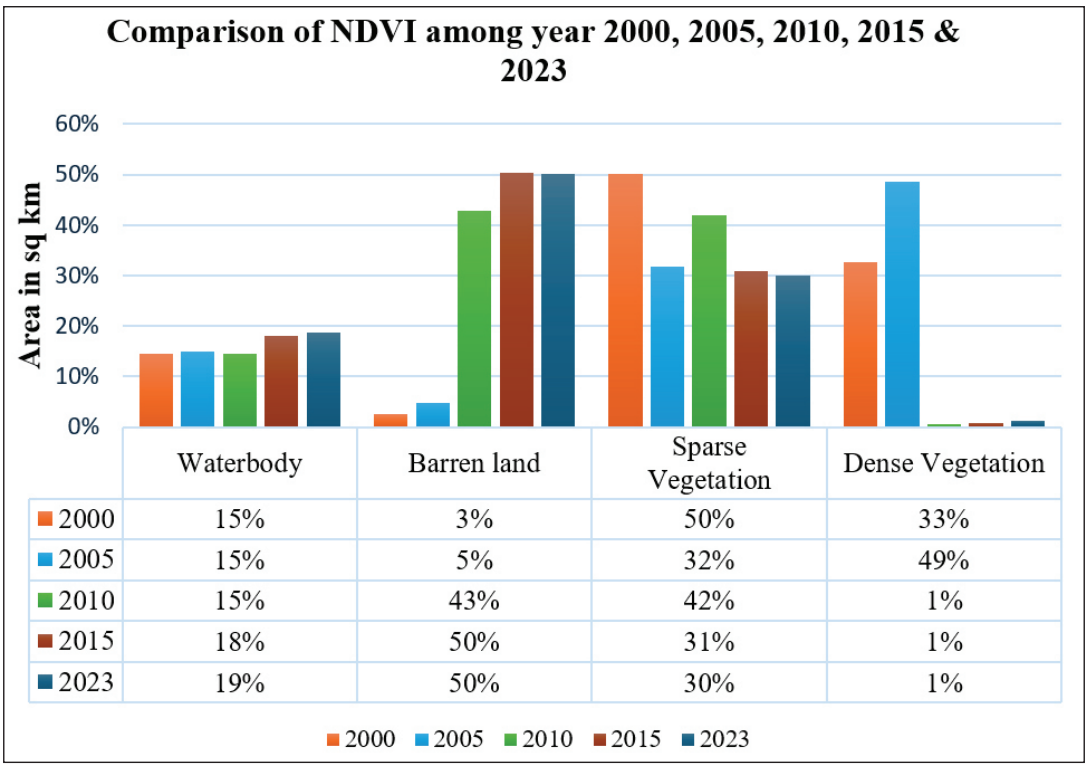

Figure 6: Chart Showing Changes of the NDVI Classes Among the Year 2000, 2005, 2010, 2015, and 2023

LULC Mapping based on NDWI

The purpose of NDWI calculation (Table 5) was to identify the variation in water body over the study area. So, the changes of water body have been well documented from the NDWI (Fig. 7). Two LULC types such as land (representing negative values) and water (representing positive values) have been identified using NDWI. The area coverage of the observed NDWI in each year is presented below.

From 2000 to 2023, NDWI data reveals significant shifts in water and land cover. In 2000, water-covered areas accounted for 12,831.43 km² (30% of the total area), while land covered 29,421.75 km² (70%). By 2005, water areas decreased to 10,258.06 km² (24%), with land expanding to 32,003.49 km² (76%). This trend continued in 2010, with water further reducing to 7,372.70 km² (17%) and land increasing to 34,962.89 km² (83%). In 2015, water-covered areas dropped to 4,696.48 km² (11%), while land reached 38,081.36 km² (89%). By 2023, water areas declined significantly to 2,462.54 km² (6%), with land covering 40,317.67 km² (94%). These changes (Fig. 8) suggest notable environmental shifts or land use changes over time.

Table 5: NDWI Classes for the Five Years with Area

Year	Area in km²		Area in Percentage	
	Water	**Land**	**Water**	**Land**
2000	12831.43	29421.75	30	70
2005	10258.06	32003.49	24	76
2010	7372.701	34962.89	17	83
2015	4696.479	38081.36	11	89
2023	2462.535	40317.67	6	94

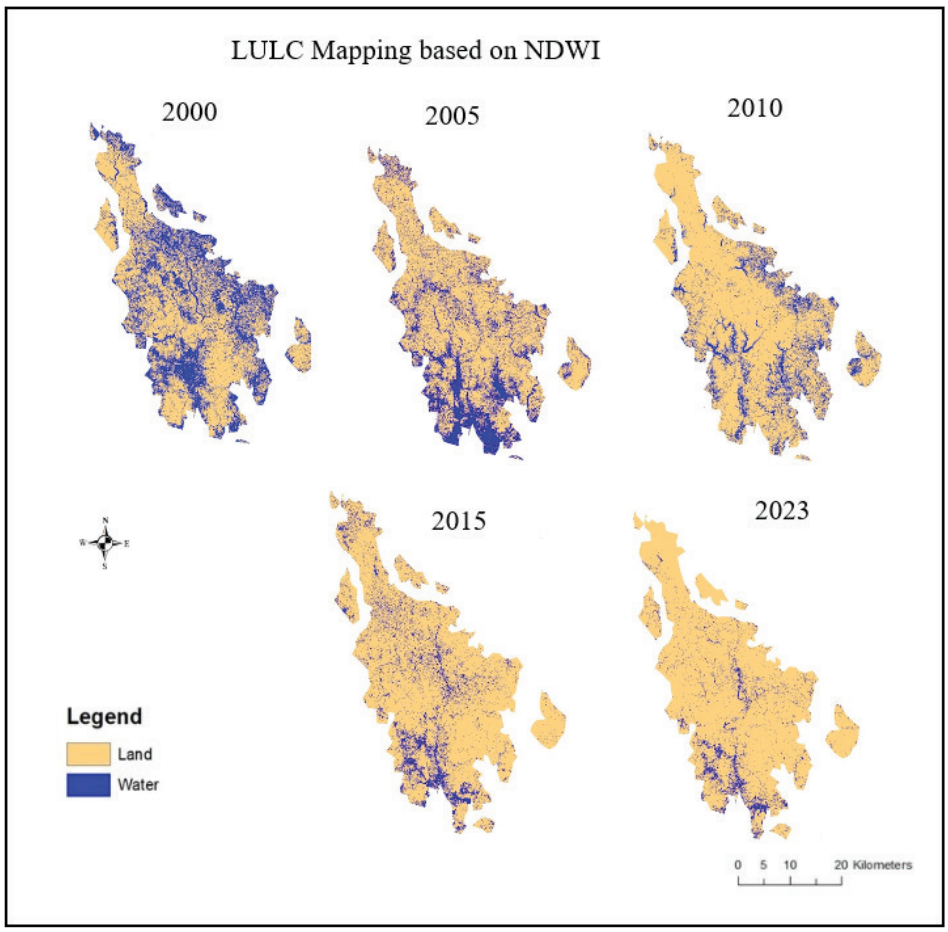

Figure 7: Landuse-Landcover (LULC) Map of the Research Area Using NDWI Classification (2000, 2005, 2010, 2015 & 2023)

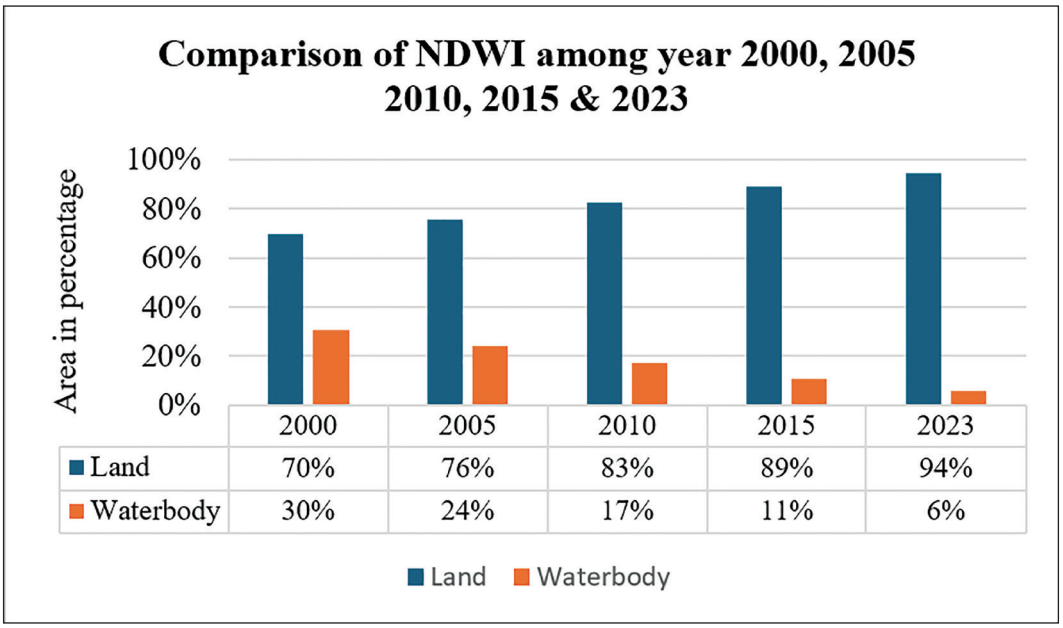

Figure 8: Chart Showing Changes of the NDWI Classes Among Year 2000, 2005, 2010, 2015, and 2023

LULC Mapping based on NDBI

The Normalized Difference Built-up Index (NDBI) is used to detect and monitor urban areas by differentiating built-up surfaces from other land types in satellite imagery. It helps track urban growth; map developed areas and classify land cover more accurately. The Normalized Difference Built-up Index (NDBI) for the years 2000, 2005, 2010, 2015, and 2023 provides insights into the changing dynamics of built-up areas within the region (Fig. 8). In 2000, the maximum NDBI value was 0.537 (Table 6), indicating the highest concentration of built-up areas, while the minimum value was -0.319, representing regions with minimal or no built-up activity. The mean NDBI was 0.109, with a standard deviation of 0.61, reflecting significant variability in built-up levels. By 2005, the maximum NDBI decreased to 0.382, and the minimum increased to -0.384, with a mean of -0.001 and a standard deviation of 0.54, indicating a reduction in average built-up concentration and moderate variability. In 2010, a notable increase in the maximum NDBI to 0.594 was observed, indicating intensified built-up activity, while the minimum NDBI dropped to -0.686. The mean value further decreased to -0.046, and the standard deviation narrowed to 0.091, suggesting a concentration of values around non-built-up areas.

In 2015, the maximum NDBI decreased to 0.418, and the minimum value rose slightly to -0.390, with the mean increasing to 0.014, indicating a mild recovery in built-up concentration. The standard deviation of 0.57 suggested persistent variability. By 2023, the maximum NDBI value further declined to 0.367, while the minimum increased to -0.415, with a mean of -0.024 and a standard deviation of 0.55, reflecting moderate dispersion. These statistical trends demonstrate the temporal variations in built-up area concentration, highlighting shifts in urbanization patterns and land development dynamics across the region from 2000 to 2023. The fluctuations in NDBI values illustrate the impact of urban expansion, land use changes, and environmental factors on the built-up landscape over time.

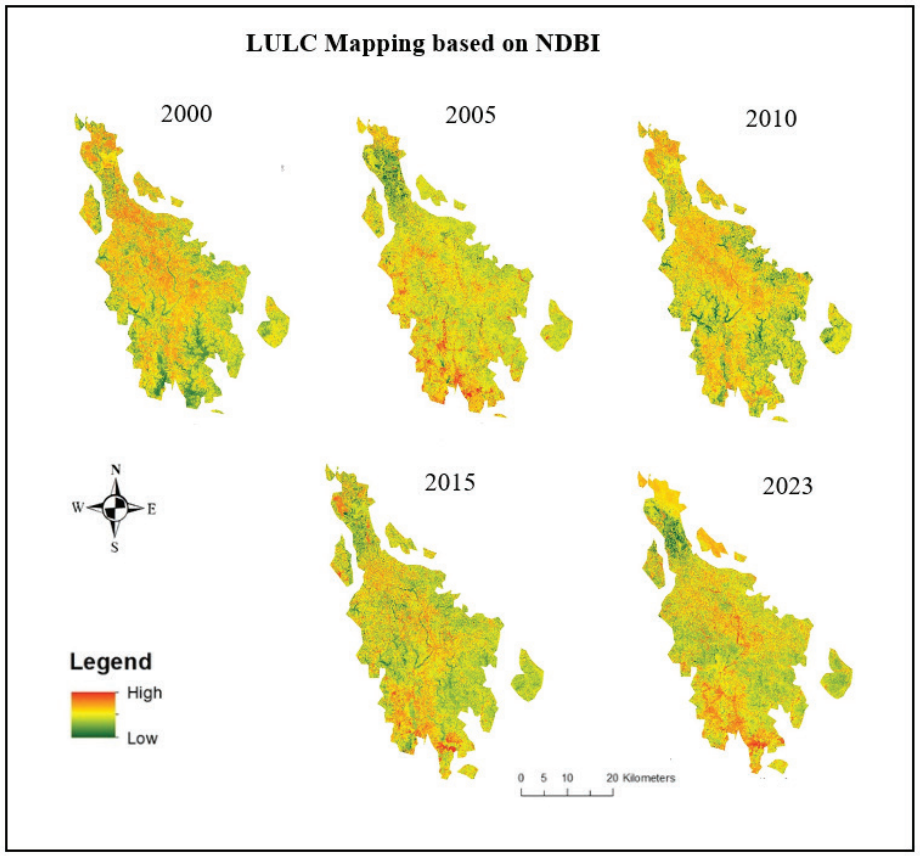

Figure 9: Landuse-Landcover (LULC) Map of the Research Area Using NDBI Classification (2000, 2005, 2010, 2015 & 2023)

Table 6: Maximum, Minimum, Mean and Standard deviation values of NDBI

Values/Years	2000	2005	2010	2015	2023
Maximum	0.536991	0.382376	0.59375	0.417668	0.36697
Minimum	-0.31903	-0.38435	-0.68628	-0.39046	-0.4153
Mean	0.10898	-0.00099	-0.04626	0.01361	-0.02416
Standard deviation	.61	0.54	0. 091	0.57	.55

DISCUSSION

The spatiotemporal analysis of land use and land cover (LULC) changes in the Madhupur Tract region from 2000 to 2023, based on NDVI, NDWI, and NDBI indices derived from Landsat imagery, reveals significant landscape shifts driven by rapid urbanization. These changes highlight the region's vulnerability as a Pleistocene uplifted terrain and underscore the need to examine their drivers, environmental impacts, and the robustness of the methods employed.

The NDVI results show a marked decline in vegetation cover, with dense vegetation dropping from 13,810.3 km² in 2000 to 551 km² in 2023, a loss of over 96%. This mirrors the unsupervised classification findings, where forest cover decreased from 29% to 11% over the same period. Meanwhile, barren land surged from 1,098.8 km² to 21,455.7 km², indicating a transition to degraded or developed surfaces. These trends align with prior observations of deforestation in the Madhupur Sal Forest and settlement growth, likely driven by population pressures and industrial expansion, such as garment factories. Our 96% vegetation loss exceeds the 23.35% forest decline reported over 30 years elsewhere in the region, suggesting an accelerated trend in this study period. The NDBI analysis supports this, showing a peak in built-up activity in 2010 (maximum NDBI of 0.594), followed by a steady rise in settlement areas from 10% (4,181.72 km²) to 30% (12,524 km²) by 2023. This urban sprawl appears to be the primary force behind vegetation loss and land degradation.

The NDWI analysis reveals a drastic reduction in water bodies, falling from 12,831.43 km² (30%) in 2000 to 2,462.54 km² (6%) in 2023,an 80% decline. This contrasts with the unsupervised classification, which suggests a slight increase in water coverage (20% to 22%), pointing to potential methodological differences. The NDWI trend likely reflects urban encroachment, such as filling water bodies for development, and possibly climate-related drying of river channels, both noted as challenges in the region. This loss threatens water availability, agricultural productivity, and ecosystem stability, amplifying environmental stress.

These LULC shifts carry significant ecological consequences. The decline in forests and vegetation reduces the region's capacity to store carbon, while the growth of built-up areas intensifies the urban heat island effect and surface temperature changes. The increase in barren land, possibly tied to erosion of the area's reddish soils, further degrades soil fertility and water retention. For example, deforestation (NDVI) reduces infiltration, shrinking water bodies (NDWI), which urban expansion (NDBI) then exploits, limiting agricultural water access and driving further settlement growth. Together, these changes suggest a cycle where urbanization accelerates environmental degradation, limiting the region's resilience to broader climate pressures.

The unsupervised classification method employed in this study offers practical benefits but also presents limitations worth considering. Its primary advantage lies in its applicability when field-specific training data are scarce, as was the case here, allowing spectral clustering to map LULC without predefined signatures. This approach achieved an overall accuracy of 92% and a Kappa coefficient of 0.825 for 2023, suggesting reliable performance for broad land cover categories like water bodies and settlements (both 90% user's accuracy). However, compared to supervised techniques, which use ground-truth data to refine class boundaries, unsupervised methods may struggle with nuanced distinctions, as seen in the lower producer's accuracy for agricultural land (58%) and bare land (53%). These discrepancies, possibly due to spectral overlap between sparse vegetation and degraded surfaces, align with challenges noted in similar studies where unsupervised classification was used without extensive validation. Moreover, the absence of field validation in this study limits the ability to confirm these classifications against real-world conditions, a gap that future research should address to enhance accuracy and credibility.

Methodologically, the use of NDVI, NDWI, and NDBI provides a solid basis for tracking LULC dynamics, with the 2023 classification demonstrating strong overall reliability. However, lower accuracy for certain classes indicates possible misclassification, and the five-year intervals (2000, 2005, 2010, 2015, 2023) might miss short-term shifts, such as seasonal vegetation changes or rapid urban developments. Additionally, the study's focus on remote sensing indices excludes socioeconomic factors like population growth, industrial policies, or waste generation that are likely shaped these patterns. Incorporating field surveys or more frequent satellite data could address these gaps and enhance resolution.

In summary, the Madhupur Tract's LULC changes reflect a region undergoing rapid transformation, with urbanization driving significant losses in forests, water bodies, and vegetation health. These findings highlight the need for sustainable land management to mitigate ecological impacts, while the methodological limitations suggest avenues for refining future research. This analysis offers valuable insights for balancing development with environmental conservation in the region.

CONCLUSIONS

This study comprehensively investigates the spatiotemporal dynamics of land use and land cover (LULC) changes in the Madhupur Tract region of Bangladesh from 2000 to 2023, using geospatial tools and Landsat imagery. The findings reveal profound landscape transformations driven by rapid and unplanned urbanization. The most notable trend is the sharp decline in forest cover, which has plummeted from 29% of the area in 2000 to just 11% in 2023. This alarming deforestation is primarily a result of expanding urban areas, infrastructure projects, and other human activities, posing severe risks to biodiversity, climate regulation, and ecosystem services.

In parallel, settlement areas have surged dramatically, increasing from 10% in 2000 to 30% in 2023. This rapid urbanization has not only contributed to the loss of natural landscapes but has also intensified issues such as the urban heat island effect, air pollution, and water scarcity. The NDVI analysis further highlights the degradation of vegetation health, while the significant rise in barren land emphasizes the growing environmental stress on the region's ecosystems. The NDWI results reveal a concerning decline in water bodies, underscoring the vulnerability of the area to hydrological imbalances and water shortages. The NDBI analysis confirms the increasing footprint of urban areas, reflecting the region's rapid urban growth and its accompanying environmental pressures. Collectively, these findings provide critical data for policymakers, urban planners, and environmental managers, offering an empirical foundation for making informed decisions regarding sustainable urban development and environmental conservation.

In conclusion, this study underscores the urgent need for sustainable land management practices, urban planning policies, and conservation initiatives to mitigate the adverse environmental impacts of rapid urbanization in the Madhupur Tract. By recognizing the scale and nature of LULC changes, decision-makers can implement strategies to preserve ecological integrity, promote resilient urban growth, and secure a sustainable future for the region's ecosystems and communities.

ACKNOWLEDGEMENT

Authors are gratefully acknowledged the USGS earth exploratory archives for providing the satellite images with free of cost.

REFERENCES

Adegboyega, S. A., Oloukoi, J., Olajuyigbe, A. E., 2019. Evaluation of unsustainable land use/land cover change on ecosystem services in coastal area of Lagos State, Nigeria. Applied Geomatics 11(1), 97–110. https://doi.org/10.1007/s12518-018-0242-2.

Akinci, H., Özalp, A.Y., Turgut, B., 2013. Agricultural land use suitability analysis using GIS and AHP technique. Comput Electron Agric 97:71–82.

Alam, A. K., Khan, M. S. H., 2022. Geomorphology of Bangladesh and potential land use. In Bangladesh Geosciences and Resources Potential (pp. 355-398). CRC Press.

Al Faruq, M. A., Zaman, S., Katoh, M., 2016. Analysis of forest cover changes using Landsat satellite imagery: a case study of the Madhupur Sal forest in Bangladesh. Journal of Forest Planning 21(2), 29-38.

Borges, C. K., de Medeiros, R. M., Ribeiro, R. E., dos Santos, É. G., Carneiro, R. G., dos Santos, C. A., 2016. Study of biophysical parameters using remote

sensing techniques to Quixeré-CE region. Journal of Hyperspectral Remote Sensing 6(6), 283–294.

Carlson, T. N., Ripley, D. A., 1997. On the relation between NDVI, fractional vegetation cover, and leaf area index. Remote Sensing of Environment 62(3), 241–252.

Chaurasia, R., Closhali, D.C., Dhaliwal, S.S., Sharma, P.K.M., Kudrat, M., Tiwari, A.K., 1996. Landuse change analysis for agricultural management: a study of Tehsil Tal-wandi Sabo, Punjap. J. Indian Soc. Remote Sens. 24: 115-123.

Chen, X. L., Zhao, H. M., Li, P. X., Yin, Z. Y., 2006. Remote sensing image-based analysis of the relationship between urban heat island and land use/cover changes. Remote Sensing of Environment 104(2), 133–146.

Ding, H., Shi, W., 2013. Land-use/land-cover change and its influence on surface temperature: a case study in Beijing City. International Journal of Remote Sensing 34(15), 5503–5517.

Dissanayake, S., Asafu-Adjaye, J., Mahadeva, R., 2017. Addressing climate change cause and effect on land cover and land use in South Asia. Land Use Policy 67, 352-366.

Disperati, L., Virdis, S., 2015. Assessment of land-use and land-cover changes from 1965 to 2014 in Tam Giang-Cau Hai Lagoon, central Vietnam. Appl Geogr 58:48–64.

Edenhofer, O. (Ed.)., 2015. Climate change 2014: mitigation of climate change (Vol. 3). Cambridge University Press.

Gandhi, G. M., Parthiban, S., Thummalu, N., Christy, A., 2015. NDVI: Vegetation change detection using remote sensing and GIS – A case study of Vellore District. Procedia Computer Science 57, 1199–1210.

Islam, M. Y., Nasher, N. R., Karim, K. R., Rashid, K. J., 2023. Quantifying forest land-use changes using remote-sensing and CA-ANN model of Madhupur Sal Forests, Bangladesh. Heliyon 9(5).

Islam, K. K., Jose, S., Tani, M., Hyakumura, K., Krott, M., Sato, N., 2015. Does actor power impede outcomes in participatory agroforestry approach? Evidence from Sal forests area, Bangladesh. Agroforestry Systems 89, 885-899.

Luck, M., Wu, J., 2002. A gradient analysis of urban landscape pattern: A case study from the Phoenix metropolitan region, Arizona, USA. Landscape Ecology 17, 327–339. https://doi.org/10.1023/A:1020512723753.

McFeeters, S. K., 1996. The use of the normalized difference water index (NDWI) in the delineation of open water features. International Journal of Remote Sensing 17(7), 1425–1432.

Miller, A.B., Bryant, E.S., Birnie, R.W., 1998. An analysis of land cover changes in the northern forest of new England using multi-temporal Landsat MSS data. Int. J. Remote Sens. 19 (2): 215-265.

Rahman, M. M., Nishat, A., Vacik, H., 2009. Anthropogenic disturbances and plant diversity of the Madhupur Sal forests (Shorea robusta C.F. Gaertn) of Bangladesh. Journal of Forestry Research, https://doi.org/10.1080/17451590903236741.

Paolini, L., Grings, F., Sobrino, J. A., Jiménez Muñoz, J. C., Karszenbaum, H., 2006. Radiometric correction effects in Landsat multi-date/multi-sensor change detection studies. International Journal of Remote Sensing 27(4), 685-704.

Rashid, T., 2014. Holocene sea-level scenarios in Bangladesh. In Proceedings of Climate Research, https://doi.org/10.1007/978-981-4560-99-3_1.

Rouse, J. W., Haas, R. H., Schell, J. A., Deering, D. W., 1974. Monitoring vegetation systems in the great plains with ERTS. NASA Special Publication 351(1), 309.

Vermeulen, S. J., Campbell, B. M., Ingram, J. S., 2012. Climate change and food systems. Annual Review of Environment and Resources 37, 195–222.

Xu, H., 2006. Modification of normalised difference water index (NDWI) to enhance open water features in remotely sensed imagery. International Journal of Remote Sensing 27(14), 3025–3033.

Yesmin, R., Mohiuddin, A. S. M., Uddin, M. J., Shahid, M. A., 2014. Land use and land cover change detection at Mirzapur union of Gazipur district of Bangladesh using remote sensing and GIS technology. In IOP Conference Series: Earth and Environmental Science (Vol. 20, No. 1, p. 012055). IOP Publishing.